BRITTLE AND DUCTILE FAILURE UNDER MIXED MODE LOADING

D. J. Smith[1], T. D. Swankie[1], M. Ayatollahi[1], M. J. Pavier[1]

The fracture behaviour under mixed mode I and II loading of a polymer (PMMA) and several steels is examined. The three steels are; a BS1501 pressure vessel steel tested at -120^{0}C, a heat treated 3CrMo rotor steel at 20^{0}C and a A508 pressure vessel steel at 20^{0}C. The fracture results are explored in terms of loci based on the maximum tensile stress (MTS) fracture criterion and plastic collapse. In all cases the results lie either inside or on these loci.

INTRODUCTION

Investigations into mixed mode loading have generally been restricted to linear elastic materials since the theoretical analyses (1,2) are more fully understood than for elastic-plastic materials. Criteria for elastic-plastic fracture behaviour of materials for combinations of tension and shear are being developed. If brittle fracture occurs under contained yielding several researchers (3,4) suggest that an elastic-hardening plastic analysis (5) combined with the MTS criterion provides an improved description of mixed mode I/II fracture. In this paper we explore a simple approach to evaluating brittle and ductile fracture under mixed mode loading and we bring together results from a series of investigations using PMMA and several steels.

EXPERIMENTS

Mixed mode I/II loading was obtained using a recently developed test fixture and SEN specimens. The loading fixture is described in detail elsewhere, (4).

* Department of Mechanical Engineering, University of Bristol, Bristol BS8 1TR

Experiments were carried out using a polymer (PMMA) and three steels; a BS1501 pressure vessel steel, a heat treated 3CrMo rotor steel and a A508 pressure vessel steel. The BS1501 steel was tested at -120^{0}C, and the other materials tested at room temperature. The 3CrMo steel was subjected to a heat treatment to ensure brittle fracture for mode I loading. Further details of the experiments can be found elsewhere (PMMA, 4, BS1501 steel, 6 and 7, 3CrMo steel, 8 and A508 steel, 9).

The test results for all four materials are shown in Figure 1 to 4. For all combinations of tension and shear fracture in the PMMA was brittle. For the BS1501 steel, a transition from brittle (cleavage) fracture for mode I to ductile shear fracture for mode II was observed (6). Similar characteristics were observed for the 3CrMo steel, cleavage fracture in mode I and ductile shear fracture in mode II. For the PMMA, BS1501 and 3CrMo steels the tensile and shear loads at instability are shown in Figures 2 to 4 respectively. Finally for the A508 steel, ductile tearing occurred for any combination of tensile and shear loads, (9). The maximum attained tensile and shear loads are shown in Figure 4. Beyond maximum load ductile tearing resistance curves were obtained. The results are shown in Figure 5.

ANALYSIS

The analysis is confined to predicting loads for brittle fracture and plastic collapse for ductile failure. For brittle fracture it is assumed that the stress intensity factor K_{If} for failure coincides with the observed failure load for brittle fracture of the PMMA and the BS1501 and 3CrMo steels. For plastic collapse, limit load solutions based on the material flow stress σ_{fl}.

Brittle Fracture

For brittle fracture, without the presence of significant near crack tip plasticity, the maximum tangential stress (MTS) criterion of Erdogan and Sih (1) postulates that the ratio of K_{II}/K_{If} and K_I/K_{If} varies according to

$$\frac{K_I}{K_{If}}\cos^3(\theta_0/2)-\frac{3}{2}\frac{K_{II}}{K_{If}}\cos(\theta_0/2)\sin\theta_0=1 \qquad (1)$$

where θ_0 is the fracture angle that satisfies

$$K_I\sin\theta_0+K_{II}(3\cos\theta_0-1)=0 \qquad (2)$$

This criterion is plotted in Figure 2 to 5 for each material, where the tensile, N_f and shear, S_f loads for brittle fracture were determined from

$$P = K_I B\sqrt{W} / F_I(a/W, \psi);\ N_f = P\cos\psi;\ S_f = P\sin\psi \qquad (3)$$

where B is the thickness, W the width and ψ the loading angle.

Plastic Collapse

Plastic collapse conditions for combined tensile, N_L, and shear S_L, loading, assuming plane strain conditions and Tresca's yield criterion, were determined from limit load solutions summarised by Miller (10). The SEN specimens were subjected to loads through the crack tip, which would introduce a bending moment across the uncracked ligament. Plastic collapse was calculated for mixed mode loading with and without bending.

Tensile, N_L, bending M_L and shear S_L forces are related graphically by Miller in terms of their normalised values, $\tilde{n}$, $\tilde{m}$ and $\tilde{s}$, where

$$\begin{aligned} \tilde{n} &= N_L / N';\qquad & N' &= \sigma_{fl}(W-a)B \\ \tilde{m} &= M_L / 1.26M';\quad & M' &= \frac{\sigma_{fl}(W-a)^2 B}{4} \\ \tilde{s} &= S_L / S';\qquad & S' &= \frac{\sigma_{fl}(W-a)B}{2} \end{aligned} \qquad (4)$$

The locus for calculated values of N_L and S_L are shown in Fig. 1 to 4.

Without a bending component the limit load for tension and shear is given by

$$\left(\frac{N_L}{N'}\right)^2 + 1.03\left(\frac{S_L}{S'}\right) = 1 \qquad (5)$$

The curve for mixed mode plastic collapse without bending is shown in Figures 2 and 3 for the BS1501 and 3CrMo steels respectively.

CONCLUDING REMARKS

In all four materials the experiments lie either outside or on the failure loci for brittle fracture or plastic collapse (ductile fracture). For PMMA in pure shear, although failure was by brittle fracture, the two failure loci are relatively close and

some degree of plasticity in mode II is expected. In the BS1501 and 3CrMo steels there was a distinct change in failure mode. This change is predicted by the failure loci.

For failure by plastic collapse the analysis shows that a lower bound locus is obtained for combined bending and tension (M+N) compared with tension alone (N). This is shown in Figures 2 and 3. Results from finite element analysis for plastic collapse in the BS1501 steel specimens are also shown in Figure 2 and show that generally the predicted plastic collapse loci are conservative. For the A508 steel predicted loads are considerably lower than the experiments. The differing ductile tearing in this steel for mode I and mode II, Figure 5, is not reflected in the attainment of maximum load.

ACKNOWLEDGEMENTS

The financial support for this work was provided by EPSRC, grant numbers GR/F57922 and GR/K21894, and also by Nuclear Electric plc.

REFERENCES

1. Erdogan, F. and Sih, G.C., J. Basic Engineering, 85D, 1968, 519-525

2. Hellen, T.K. and Blackburn, W.S., Int. J. Fract., 11, 1975, 605-617

3. Maccagno, T.M. and Knott, J.F., Eng. Fract. Mech., 38, 2/3, 1991, 111-128

4. Davenport, J.C.W. and Smith, D.J., Fat. Fract. Engng. Mater. Struct., 16, 10, 1993, 1125-1133

5. Shih, C.F., Fracture Analysis, ASTM STP 560, 1974, 187-210

6. Swankie, T.D. Davenport, J.C.W and Smith, D.J., ICF 9, vol. 1, 1997, 207-214

7. Swankie T.D. and Smith D.J., Eng Fract. Mech to appear 1998

8. Smith D.J., Davenport J.C.W. and Swankie T.D., Int, J. Fract to appear, 1998

9. Davenport, J.C.W. and Smith, D.J., ECF10, Structural Integrity: Experiments-Models-Applications, Eds., K-H Schwalbe and C Berger, 1994, 901-910

10. Miller, A.G., Int J. Pres. Ves. & Piping, 32, 1988, 197 328

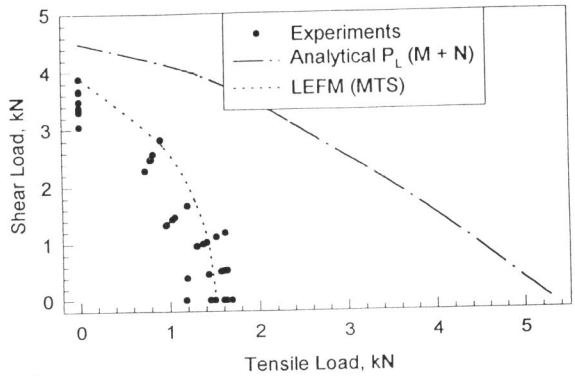

Figure 1 Fracture of PMMA at room temperature

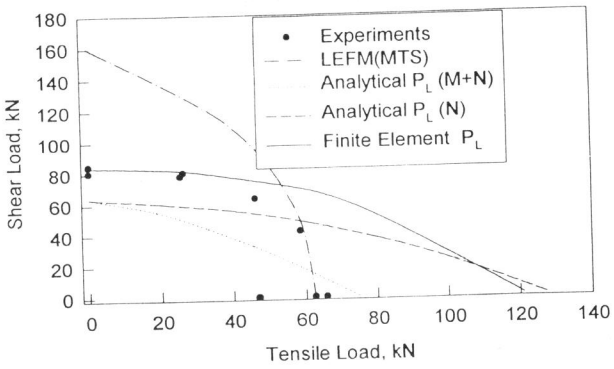

Figure 2 Fracture of BS1501 steel at -120^{0}C

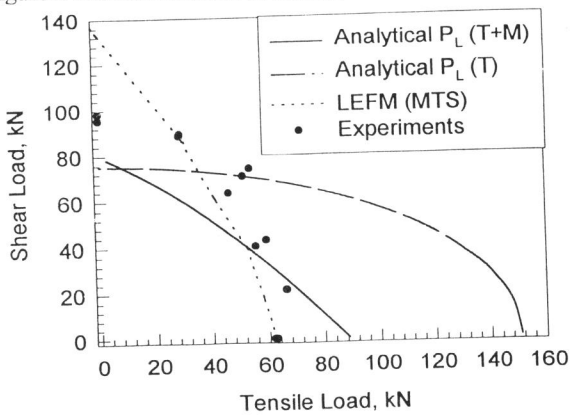

Figure 3 Fracture of 3CrMo steel at room temperature

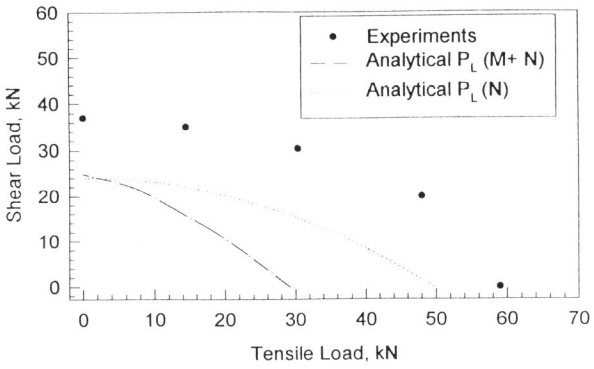

Figure 4 Fracture of A508 Steel at room temperature

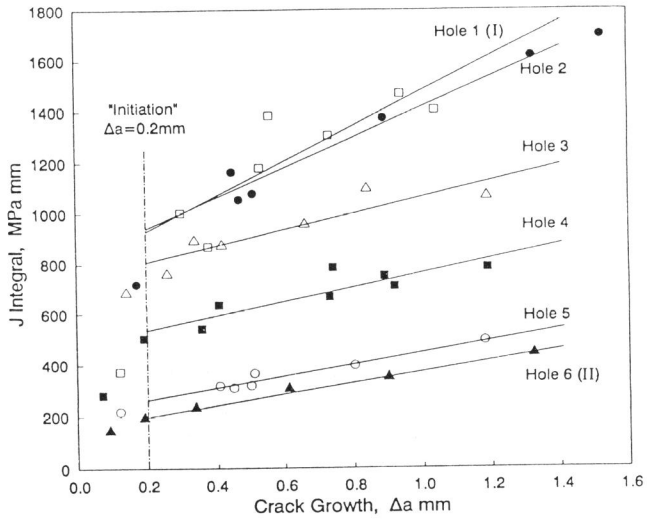

Figure 5 Ductile tearing in A508 steel at room temperature